

Diego Coppola, M. Ripepe, M. Laiolo, and C. Cigolini, 2017, Modelling satellite-derived magma discharge to explain caldera collapse: *Geology*, doi:10.1130/G38866.1.

MATERIALS AND METHODS

Space-based thermal analysis of the Holuhraun 2014-2015 eruption

MIROVA (Middle Infrared Observation of Volcanic Activity) is an automated global hot spot detection system (www.mirovaweb.it) based on near-real time ingestion of Moderate Resolution Imaging Spectroradiometer (MODIS) infrared data (Coppola *et al.* 2016). The system completes automatic detection and location of thermal anomalies, and provides a quantification of the Volcanic Radiative Power (VRP), within 1 to 4 hours of each satellite overpass. This is achieved through a hybrid algorithm (fully described in Coppola *et al.*, 2016) based on the analysis of the Middle Infrared radiance data ($\sim 3.959 \mu\text{m}$) recorded at 1-km spatial resolution, as shown in Fig. DR1. Two MODIS instruments (carried on two NASA spacecraft; Terra and Aqua) deliver approximately 4 images per day for every target volcano located at equatorial latitudes. However, due to the polar, sun-synchronous orbit, the two satellites increase their sampling time at high latitude, providing, at least 6 to 10 overpasses per day over Iceland. An example of thermal images elaborated by the MIROVA system during the Holuhraun 2014-2015 eruption is given in Fig. DR1.

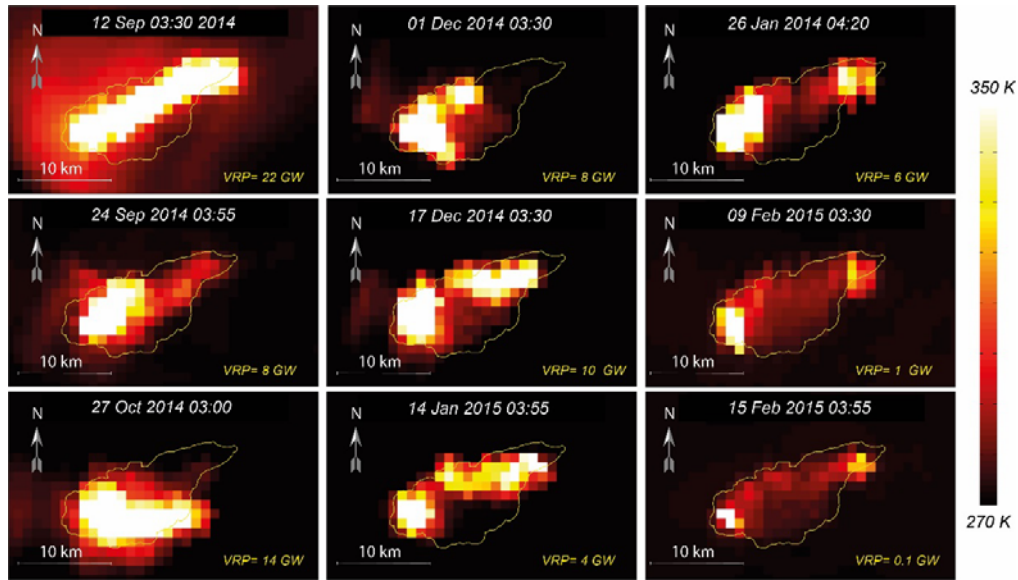


Figure DR1 – Example of selected MODIS image (brightness temperature at 3.959 μm) elaborated by the MIROVA system. Final contour of the Holuhraun 2014-2015 lava field is outlined by the yellow line.

Between August 29th, 2014 and March 4th, 2015, MIROVA detected hotspots in 1105 images over a total of 1623 MODIS overpasses above Iceland. Volcanic radiative power (VRP) ranged from ~39.1 GW, during the initial stage of the effusion, to less than 10 MW just before the end of the eruption (Figure DR2A). Following *Coppola et al. (2013)* the visual inspection of all the acquired scenes allowed us to identify a large number of images acquired in cloudy conditions, and/or under poor geometrical conditions (i.e. with high satellite zenith $> 40^\circ$) that strongly deformed and affected the thermal anomaly at ground level. We thus selected a dataset of 206 suitable images (~12.7% of the total MODIS overpasses: i.e. Fig. DR1) that has been used to provide a robust quantification of the radiant flux produced by the eruption (black circles in Figure DR2A). As a whole we estimated that the Holuhraun eruption radiated approximately 1.6×10^{17} J into the atmosphere (red curve in Fig. DR2A), with a mean radiant flux of about 10.5 GW.

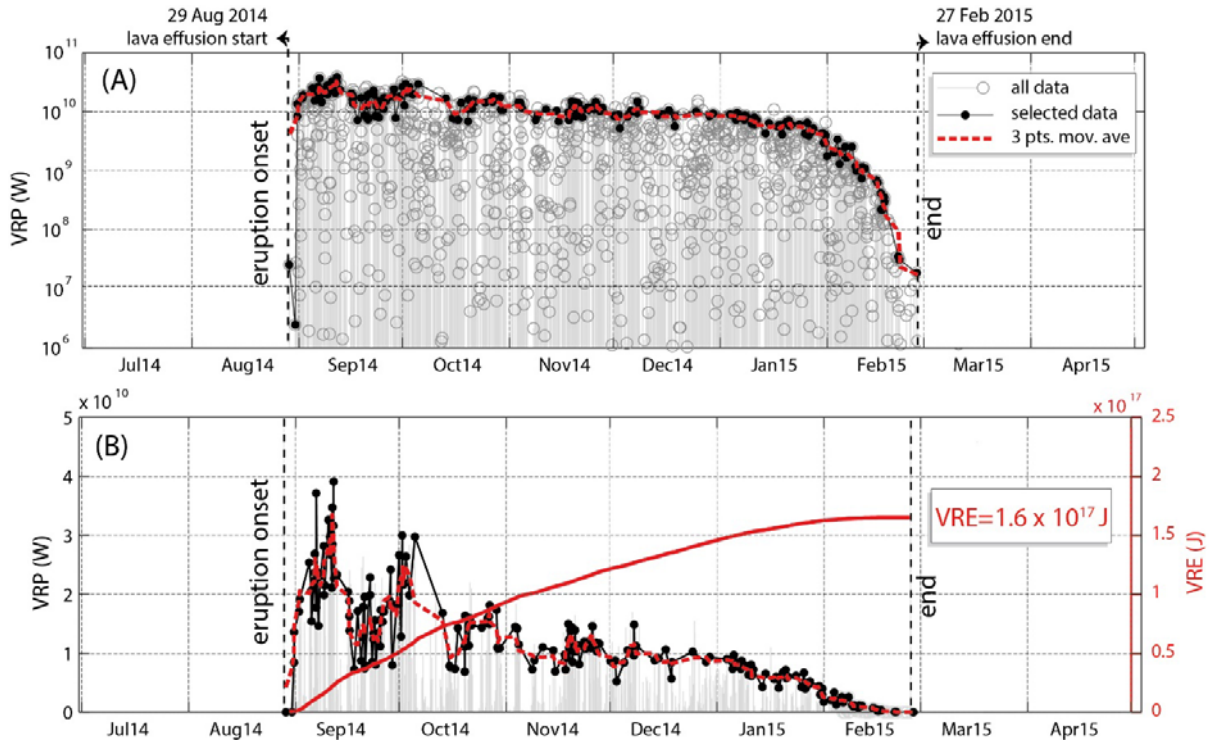


Figure DR2. Timeseries of Volcanic Radiative Power (VRP) recoded by the MIROVA system during the Holuhraun 2014-2015 eruption. (A) logarithmic scale. (B) normal scale. The cumulative radiant energy (VRE) is represented by the red thick line. Three points moving average of selected data is shown by red dashed line.

Time Averaged Lava Discharge Rate from satellite thermal data

Satellite-based thermal data have been used to estimate the lava discharge rates during effusive eruptions since 1997 (see *Harris, 2013* and references therein). This approach relies on the observed relationships between lava discharge rate, lava flow area and thermal flux (e.g. *Pieri and Baloga, 1980; Wright et al., 2001; Harris and Baloga 2009*) that become linear once an active lava flow reaches the thermal steady state (i.e after a few days for large basaltic flows; *Garel et al., 2012*). In this condition, the Time Averaged lava Discharge Rate (*TADR*), can be related to the volcanic radiant power (*VRP*) through a unique empirical parameter (c_{rad}) that takes into account the appropriate rheological, insulation and topographic conditions for the studied lava body (*Coppola et al., 2013*):

$$TADR = \frac{VRP}{c_{rad}} \quad (1)$$

where c_{rad} is the radiant density (in J m^{-3}) of the lava flow. It has been shown (Coppola et al., 2013) that the radiant density is mainly controlled by the bulk rheological properties of the active lava body. Low-viscosity basaltic lava flows exhibit the highest range of c_{rad} ($1-4 \times 10^8 \text{ J m}^{-3}$), while viscous silicic flows represent lower values ($< 1 \times 10^7 \text{ J m}^{-3}$). Coppola et al. (2013) provided an empirical method to calculate the radiant density of a lava body ($\pm 50\%$), on the basis of the silica content of erupted lavas, the latter being considered a first-order proxy of its bulk rheological properties,

$$c_{rad} = 6.45 \times 10^{25} \times (X_{SiO_2})^{-10.4} \quad (2)$$

where X_{SiO_2} is the silica content of the erupted lavas (wt. %).

For the Holuhraun basaltic lavas, we set $X_{SiO_2} = 50.5 \text{ wt\%}$ (Institute of Earth Sciences University of Iceland, 2014) which results in a calculated radiant density of $1.2 \times 10^8 \text{ J m}^{-3}$, or between 0.6 and $1.8 \times 10^8 \text{ J m}^{-3}$ considering the $\pm 50 \%$ accuracy of the empirical fit (Coppola et al., 2013). This range encompass different eruption conditions that may characterize the emplacement of the Holuhraun lava flow (i.e., channel- versus tube-fed). Accordingly, we calculated a total volume of erupted lava equal to $1.76 \pm 0.88 \text{ km}^3$, with mean values being the best estimates (Fig. DR3A).

It should be noted that a “buffering” of the thermal signal may follows rapid variations of the effusion rates (i.e. the beginning of the eruption), due the progressive and coupled evolution of radiant signal and flow area (Garel et al., 2012). This buffer reflects the time necessary to the lava flow to accommodate, in terms of flow area and radiant flux, sharp variations in effusion rate and this is essentially the reason why the highest rate was not observed during the early eruptive phase (cf. Fig. 2), but only after a transient time of several days, typical for large basaltic lava flows.

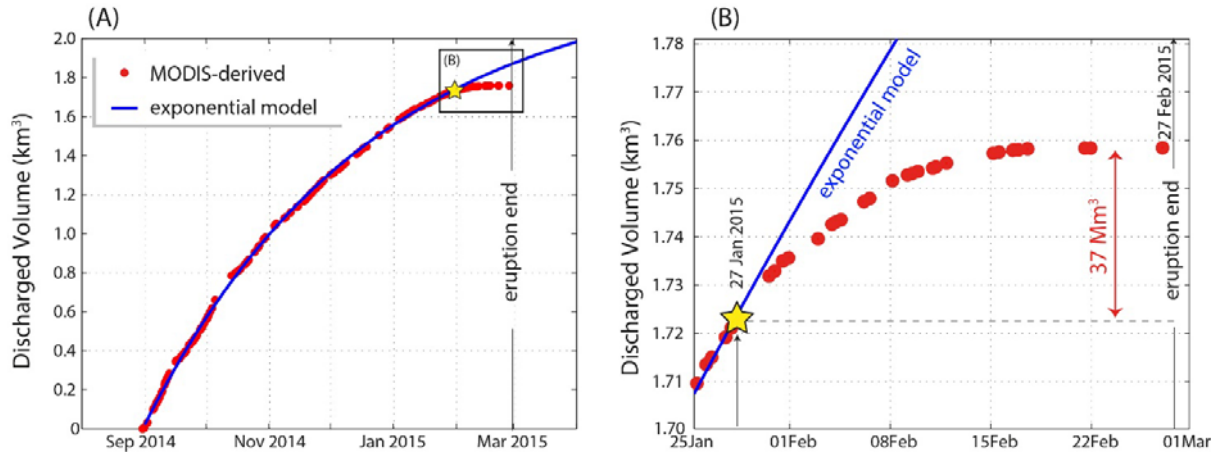
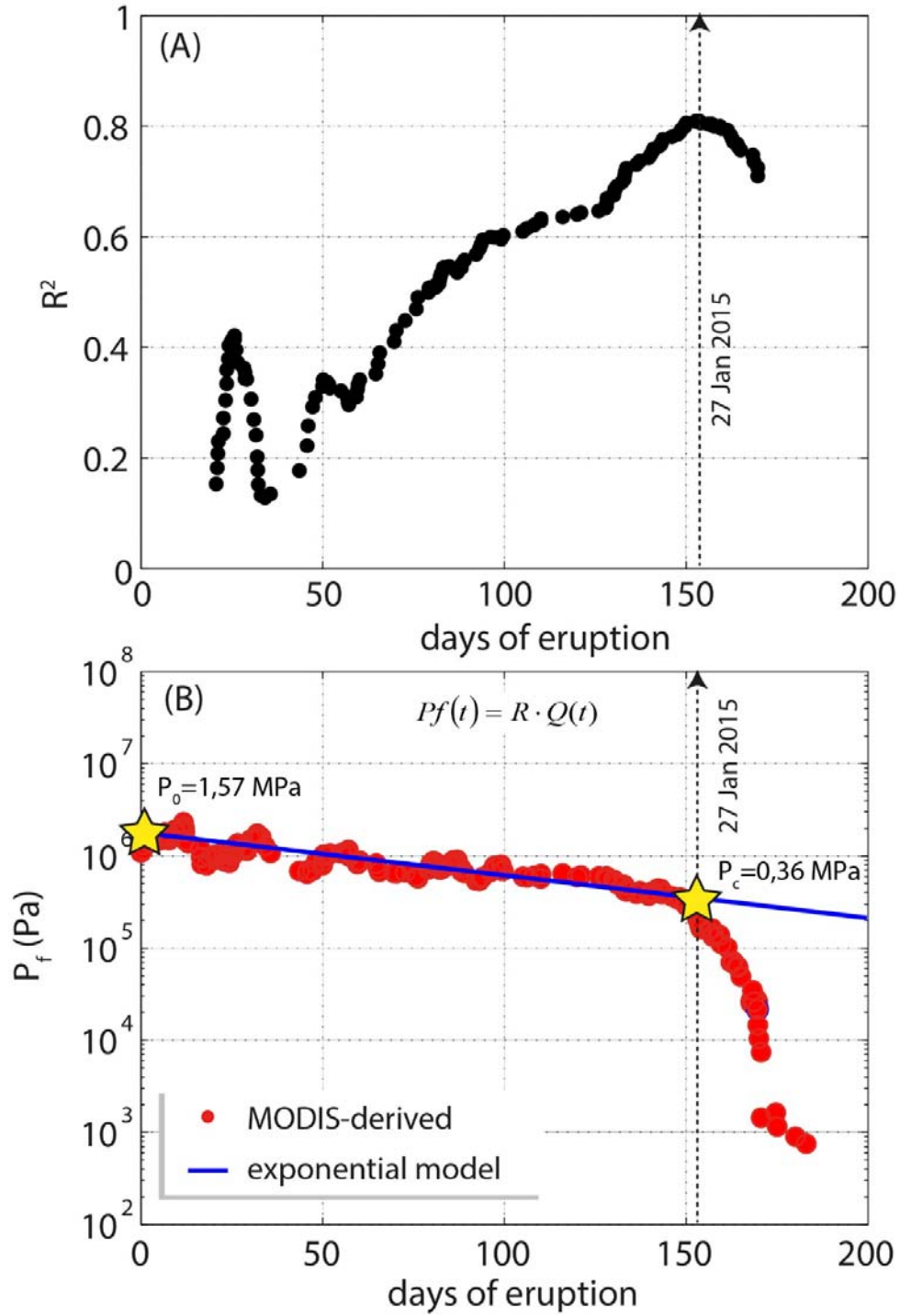


Figure DR3. (A) Magma volume discharged at the eruptive vent as derived from MODIS data (red dots) and exponential model (blue line). (B) Magma volume discharged after 27 January 27, 2015 (day 151, yellow star), when the effusion rates clearly deviated from the modelled exponential trend (blue line).

Regression analysis of eruptive trend, excess pressure and volume of the magma path

The regression coefficient (R^2) related to the exponential fit of effusion rates has been calculated by increasing progressively the number of the data samples (Fig. DR3a). Accordingly, the best fit ($R^2=0.81$) is obtained by considering the first 151 days of activity, after which effusion rates started to deviate from the exponential trend.

The MODIS-derived effusion rate data are converted into magma reservoir overpressure, P_f , by using equation 2 (Fig. DR3b). By the eruptive day 151 the overpressure has reduced to ~0,36 MPa which is ascribed to the critical value (P_c) necessary to keep the dike open. The volume erupted after this date is ~37 Mm³ (Fig. DR3B) is ascribed to the ultimate closure of the magma flow path.



87

88 **Figure DR4** – (A) Variation of regression coefficient (R^2) calculated by progressively fitting an
89 increasing number of effusion rate data. The best fit is obtained after 151 days of activity. (B)
90 Evolution of the pressure in the dike as calculated from MODIS-derive effusion rate (red dots) by
91 equation (2). Yellow stars indicate the initial excess pressure ($P_0=1.57$ MPa) and the critical
92 pressure ($P_c=0.36$ MPa) as modelled by the exponential best-fit (blue line).

ADDITIONAL REFERENCES

- Coppola, D., Laiolo, M., Piscopo, D., and Cigolini, C., 2013, Rheological control on the radiant density of active lava flows and domes: *Journal of Volcanology Geothermal Research*, v. 249, p. 39–48, doi:10.1016/j.jvolgeores.2012.09.005.
- Coppola, D., Laiolo, M., Cigolini, C., Delle Donne, D., and Ripepe, M., 2016, Enhanced volcanic hot-spot detection using MODIS IR data: results from the MIROVA system, *in* Harris, A.J.L., et al., eds., *Detecting, Modelling and Responding to Effusive Eruptions*: Geological Society, London, Special Publications, v. 426, doi: 10.1144/SP426.5. p. 181-205.
- Garel, F., Kaminski, E., Tait, S., Limare, A., 2012. An experimental study of the surface thermal signature of hot subaerial isoviscous gravity currents: implications for thermal monitoring of lava flows and domes. *Journal of Geophysical Research* 117, B02205. <http://dx.doi.org/10.1029/2011JB008698>.
- Harris, A.J.L., and Baloga, S., 2009, Lava discharge rates from satellite-measured heat flux: *Geophys. Res. Lett.*, v. 36, p. L19302, doi:10.1029/2009GL039717.
- Harris, A.J.L., 2013, *Thermal Remote Sensing of Active Volcanoes: A User's Manual*. ISBN: 9780521859455.
- Harris, A.J.L., and Baloga, S., 2009, Lava discharge rates from satellite-measured heat flux: *Geophys. Res. Lett.*, v. 36, p. L19302, doi:10.1029/2009GL039717.
- Institute of Earth Sciences University of Iceland, 2014, Internal Report: http://earthice.hi.is/chemical_composition_basalt_erupted_29_august_2014_through_1797ad_holuhraun_linear_vent_system_north. [Last accessed: 20 January 2017.]]
- Pieri, D.C., Baloga, S.M., 1986. Eruption rate, area, and length relationships for some Hawaiian lava flows. *Journal of Volcanology and Geothermal Research* 30, 29–45.
- Wright, R., Blake, S., Harris, A.J.L., and Rothery, D.A., 2001, A simple explanation for the space-based calculation of lava eruption rates: *Earth Planetary and Science Letters*, v. 192, p. 223 – 233, doi: 10.1016/S0012-821X(01)00443-5.